

Coupling mode-destination accessibility with seismic risk assessment to identify at-risk communities

MAHALIA MILLER*

mahalia@alum.mit.edu

JACK W. BAKER†

bakerjw@stanford.edu

Abstract

In this paper, we develop a framework for coupling mode-destination accessibility with quantitative seismic risk assessment to identify communities at high risk for travel disruptions after an earthquake. Mode-destination accessibility measures the ability of people to reach destinations they desire. We use a probabilistic seismic risk assessment procedure, including a stochastic set of earthquake events, ground-motion intensity maps, damage maps, and realizations of traffic and accessibility impacts. For a case study of the San Francisco Bay Area, we couple our seismic risk framework with a practical activity-based traffic model. As a result, we quantify accessibility risk probabilistically by community and household type. We find that accessibility varies more strongly as a function of travelers' geographic location than as a function of their income class, and we identify particularly at-risk communities. We also observe that communities more conducive to local trips by foot or bike are predicted to be less impacted by losses in accessibility. This work shows the potential to link quantitative risk assessment methodologies with high-resolution travel models used by transportation planners. Quantitative risk metrics of this type should have great utility for planners working to reduce risk to a region's infrastructure systems.

I. INTRODUCTION

Seismic risk assessment in earthquake engineering tends to focus on buildings, bridges, and the performance of infrastructure systems. For measuring the performance of transportation systems, researchers typically use engineering-based metrics such as the post-earthquake connectivity loss, which quantifies the decrease in the number of origins or generators connected to a destination node [e.g., 1], or the post-earthquake travel distance between two locations of interest [e.g., 2]. These frameworks have provided insight into seismic vulnerability and possible risk mitigation, but do not directly quantify ramifications for people.

In the field of vulnerability sciences, researchers have long stressed the importance of the impact on human welfare from earthquakes. For example, Bolin and Stanford write that, "Natural disasters have more to do with the social, political, and economic aspects than they do with the environmental hazards that trigger them. Disasters occur at the interface of vulnerable people and hazardous environments" [3]. A recent World Bank and United Nations report echoed this idea that the effects on human welfare turn natural hazards into disasters [4]. Historical events demonstrate the complex social effects of earthquakes. For example, on one hand the 1994

*Corresponding author: Phone: +1-617-692-0574. Department of Civil and Environmental Engineering, Stanford University, 473 Via Ortega, MC 4020, Stanford, CA 94305, United States. Current address: Google, 345 Spear St., Floor 4, San Francisco, CA 94114, United States.

†Department of Civil and Environmental Engineering, Stanford University, 473 Via Ortega, MC 4020, Stanford, CA 94305, United States. URL: web.stanford.edu/~bakerjw/

16 Northridge earthquake caused major damage to nine bridges, which, while significant, represented
17 only 0.5% of the bridges estimated by Caltrans to have experienced significant shaking [5]. On
18 the other hand, over half of businesses reported closing after the earthquake, with 56% citing the
19 "inability of employees to get to work" as a reason [6]. Furthermore, the total economic cost of
20 transport-related interruptions ("commuting, inhibited customer access, and shipping and supply
21 disruptions") from this earthquake is estimated at 2.16 billion USD (2014) [7], using the consumer
22 price index to account for inflation.

23 Some researchers have measured the impact of earthquakes on transportation infrastructure
24 using the cumulative extra time needed for travel due to damage, sometimes called travel time
25 delay [e.g., 8, 9]. This performance measure captures basic re-routing due to road closures and
26 identifies roads more likely to be congested. Travel time approximately measures impact on people,
27 but does not capture the fact that some destinations and trips have higher value than others. It
28 also focuses on aggregate regional effects rather than individual communities and demographic
29 groups. Others have considered the qualitative criteria-based metric "disruption index" [10], but
30 this does not provide a quantitative link between physical damage to infrastructure and resulting
31 human ramifications. Other work has looked at resiliency, but defined it in pure engineering
32 terms, such as percentage of a road network that is functional [11]. Outside of transportation
33 systems, some researchers have investigated the interplay between earthquake damage to the
34 electric power and wastewater networks, and the usability of houses and other buildings [12].

35 In contrast to the work on transportation-related seismic risk, urban planning has a long
36 tradition of studying the impact on people of events and policy [13]. Accessibility is one popular
37 metric to measure the impact of different transportation network scenarios, and it measures how
38 easily people can get to desirable destinations, which is one measure of social impact [14]. Within
39 urban planning, accessibility has been measured in many ways, including individual accessibility,
40 economic benefits of accessibility, and mode-destination accessibility [15]. The mode-destination
41 accessibility is computed by taking the log value of the sum of a function of the utilities of each
42 destination over all possible destinations and travel modes, where the utility decreases if getting
43 to that destination is more costly or time-intensive [16]. This choice of accessibility definition is
44 particularly useful for quantifying the impacts of disasters such as earthquakes, because certain
45 destinations might be more critical for people in certain locations or from certain socio-economic
46 groups. However, this accessibility measure has not previously been linked to risk assessment. In
47 addition, the majority of work to date assumes that travel demand and mode choice will remain
48 unchanged after a future earthquake, which historical data suggests is not the case [7]. A first step
49 towards considering variable demand is work in the literature that varies demand by applying a
50 constant multiplicative factor on all pre-earthquake travel demand [8], but again this approach
51 lacks any resolution at the geographic or socio-economic level.

52 In this paper, we develop a framework for coupling mode-destination accessibility with a
53 quantitative seismic-risk assessment to identify at-risk populations and measure the accompanying
54 impacts on human welfare. We illustrate our approach with a case study of the San Francisco Bay
55 Area transportation network, including highways, local roads, and public transportation lines.
56 This study analyzes a set of forty hazard-consistent earthquake scenarios, ground-motion intensity
57 maps, and damage maps, as introduced in [17, 18]. For each of these damage maps, we model
58 damage with an agent-based transportation model used by the local transportation authorities
59 that considers the impacts of damage to bridges, roads, and transit lines, and captures variable
60 user demand. Then, with this model, we estimate losses in accessibility for 12 socio-economic
61 groups and for a number of communities within the study region.

62

II. CASE STUDY: SAN FRANCISCO BAY AREA

63 We consider the San Francisco Bay Area to illustrate our approach (Figure 1). This seismically
 64 active area follows a polycentric metropolitan form, with San Francisco as the primary center
 65 and other jobs concentrated in suburban centers such as San Jose [19]. The region has a wide
 66 array of trip patterns for mandatory and non-mandatory trips. Furthermore, trip times and routes
 67 vary greatly depending on travel preferences and workplace locations [19]. Thus, there may be
 68 noticeable disparities among households in the risk of travel-related impacts due to earthquakes.

69 This analysis considers the complex web of roads and transit networks of the case study
 70 area. The roads are modeled by a directed graph $G = (V, E)$, where V is a finite set of vertices
 71 representing intersections, and the set E , whose elements are edges representing road links, is
 72 a binary relation on V . In this model, $(|V|, |E|) = (11,921, 32,858)$ including centroidal links and
 73 $(|V|, |E|) = (9,635, 24,404)$ without. Centroidal links do not correspond to particular physical roads
 74 but instead capture flows of people from outside the study area or from some minor local roads.
 75 Forty-three transit networks such as bus, light rail and ferry systems are also modeled. We model
 76 potential damage to 1743 highway bridges impacting the road and some transit networks, and
 77 1409 structures impacting the rapid transit network, BART. Details of the seismic risk calculations
 78 for this network are provided in the following subsections.

79 I. Ground-motion intensity maps

80 I.1 Theory

81 We now describe how to produce a set of maps with ground-motion intensity realizations at
 82 each location of interest, and corresponding occurrence rates that reasonably capture the joint
 83 distribution of the ground-motion intensity at all locations of interest throughout the region [e.g.,
 84 20]. First, we generate Q earthquake scenarios from a seismic source model, which specifies the
 85 rates at which earthquakes of various magnitudes, locations, and faulting types will occur. This
 86 set of earthquake scenarios is comparable to a stochastic event catalogue in the insurance industry.

87 Second, for each earthquake scenario in the seismic source model, we use an empirical ground-
 88 motion prediction equation (GMPE) to predict the log mean and standard deviation of a ground
 89 motion intensity measure at each location of interest. Then, for each of the Q earthquake scenarios,
 90 we sample b realizations of spatially correlated ground-motion intensity residual terms. The total
 91 log ground-motion intensity (Y) for a given realization is computed as

$$\ln Y_{ij} = \overline{\ln Y(M_j, R_{ij}, V_{s30,i}, \dots)} + \sigma_{ij}\epsilon_{ij} + \tau_j\eta_j \quad (1)$$

92 where $\overline{\ln Y(M_j, R_{ij}, V_{s30,i}, \dots)}$ is the predicted mean log ground motion intensity at location index
 93 i , given an earthquake of magnitude M_j at a distance of R_{ij} , observed at a site with average shear
 94 wave velocity down to 30m of $V_{s30,i}$. Variability in ground motion intensity about this mean value
 95 is represented by σ_{ij} and τ_j , the within- and between-event standard deviations, respectively, for
 96 earthquake scenarios at the index $q = 1, \dots, Q$. The index j indicates the ground-motion intensity
 97 map ($j = 1, \dots, m$ where $m = Q \times b$), ϵ_{ij} is a normalized within-event residual representing
 98 location-to-location variability and η_j is the normalized between-event residual. Both ϵ_{ij} and η_j
 99 are normal random variables with zero mean and unit standard deviation. The vector of ϵ_{ij} has a
 100 multivariate normal distribution and η_j is univariate.

101 The result is a set of m ground-motion intensity maps (e.g., Figure 2a). Since we simulate
 102 an equal number (b) of ground-motion intensity maps per earthquake scenario, the annual rate
 103 of occurrence for the j^{th} ground-motion intensity map is the original rate of occurrence of the

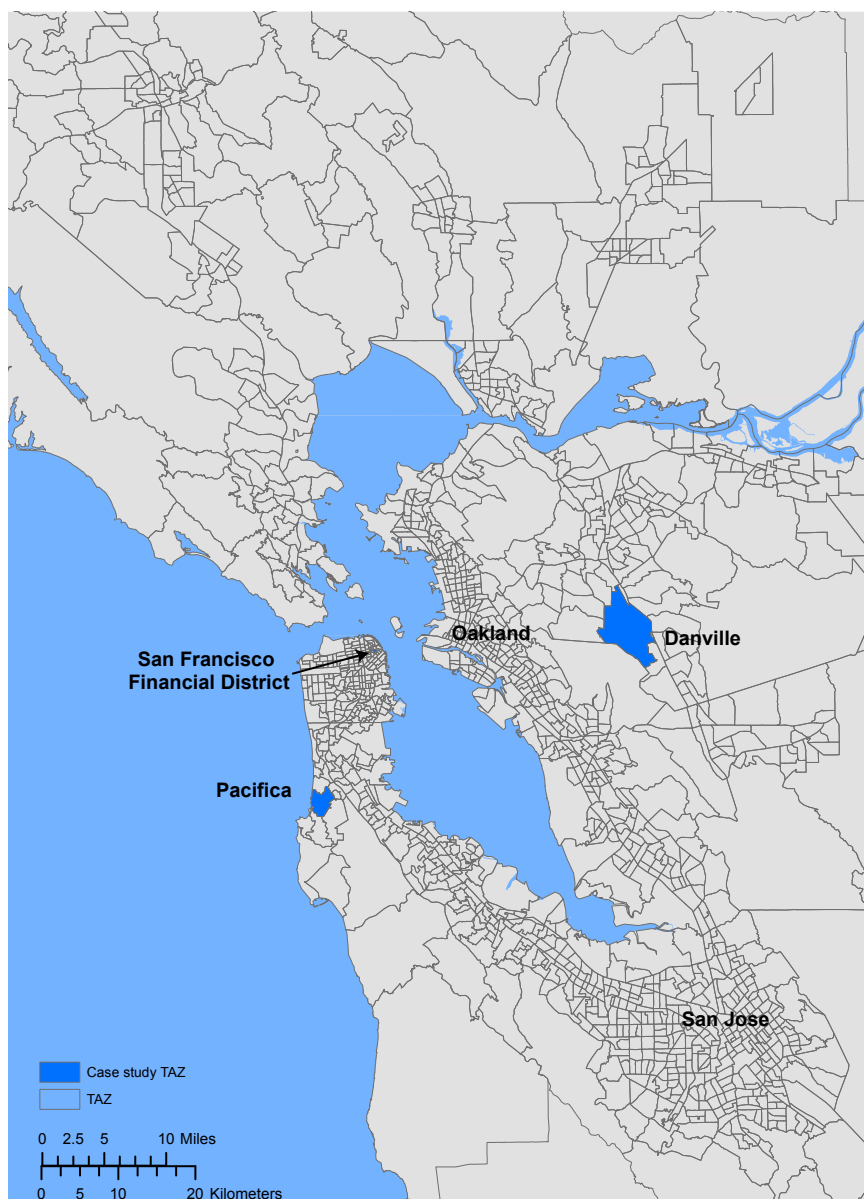


Figure 1: Travel analysis zones (TAZs) in the San Francisco Bay Area. Shading indicates the Danville, Pacifica and San Francisco Financial District TAZs that are considered in more detail below.

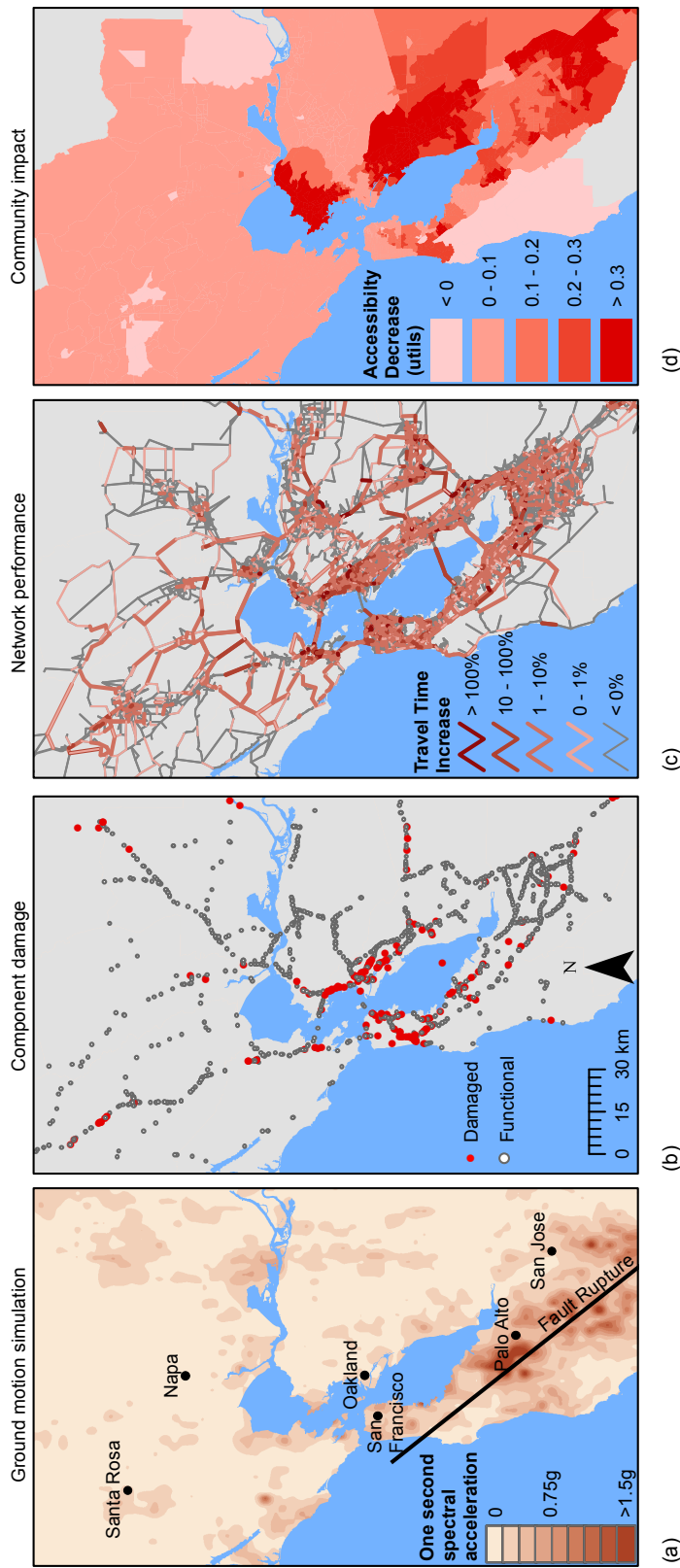


Figure 2: Illustration of the risk framework for one earthquake event including a) earthquake rupture and one-second spectral acceleration (ground motion intensity) map, b) bridge (component) damage map, c) map of travel time increase (network-performance measure) values and d) map of average accessibility decrease per travel analysis zone.

104 earthquake scenario, divided by b . We denote the occurrence rate of the j^{th} ground-motion
105 intensity map as w_j .

106 **I.2 Implementation**

107 To generate a stochastic catalog of ground-motion intensity maps, we use the OpenSHA Event Set
108 Calculator [21]. This software outputs the mean, \bar{Y}_{ij} , and standard deviation values, σ_{ij} and τ_j ,
109 for all locations of interest for a specified seismic source model and ground-motion prediction
110 equation, which are needed inputs for Equation 1. The intensity measure is the 5%-damped
111 pseudo absolute spectral acceleration (Sa) at a period $T = 1s$, which is the required input to the
112 fragility functions below. This spectral acceleration value represents the maximum acceleration
113 over time that a linear oscillator with 5% damping and a period of 1s will experience from a
114 given ground motion. We calculate these values at the location of each component (i.e., bridges
115 and other structures). Using one ground-motion intensity measure per component is a common
116 simplification that facilitates the use of fragility functions to easily predict damage to a given type
117 of structure [e.g., 9, 22]. We use the UCERF2 seismic source model to specify occurrence rates of
118 potential earthquakes in the region [23], the Wald and Allen topographic slope model to infer
119 $V_{s30,i}$ at each location [24], the Boore and Atkinson [25] ground-motion prediction equation and
120 the Jayaram and Baker model [26] for spatial correlation of ϵ_{ij} values.

121 **II. Damage maps**

122 **II.1 Theory**

123 The link between ground-motion intensity and damage to network components is provided by
124 fragility functions. Fragility functions express the probability $P(DS_i \geq ds_\zeta | Y_{ij} = y)$, where DS_i is a
125 discrete random variable representing the damage state for the i^{th} component and ds_ζ is a damage
126 state threshold of interest. The damage state is conditioned on the ground motion intensity
127 Y_{ij} having value y . We assume one component per location, and so identify both components
128 and locations via the index i . Researchers have calibrated fragility functions using historical
129 post-earthquake data [e.g., 27], experimental and analytical results [e.g., 28], hybrid approaches,
130 and expert opinion.

131 By sampling a damage state for each component, with probabilities obtained from the fragility
132 functions given the ground-motion intensity, we produce a damage map (e.g., Figure 2b). The
133 sampling process can be repeated to simulate multiple damage maps per ground-motion intensity
134 map. For example, if c damage maps are sampled per ground-motion intensity map, the occurrence
135 rates associated with the j'^{th} damage map should be adjusted accordingly to $w_{j'}$, where $w_{j'} = w_j/c$,
136 and $j' = 1, \dots, J$.

137 *Functional percentage* relationships link the component damage to the functionality of network
138 elements. For example, in a road network, when a bridge collapses, the traffic flow capacity of the
139 road it carries and it crosses are reduced to zero. These relationships are typically derived from
140 a combination of observation and expert opinion, often due to data scarcity [29]. Furthermore,
141 the relationships are typically deterministic for a certain component damage state and restoration
142 time [29]. Thus, in this paper, each damage map corresponds to a functionality state for every
143 element of the network.

¹⁴⁴ **II.2 Implementation**

¹⁴⁵ **Component damage** We use fragility functions of the following form to provide the link between
¹⁴⁶ ground-motion shaking and component damage:

$$P(DS_i \geq ds_{\xi} | Y_{ij} = y) = \Phi \left(\frac{\ln y - \lambda_{\xi,i}}{\xi_{\xi,i}} \right), \quad (2)$$

¹⁴⁷ where Φ is the standard normal cumulative distribution function, $\lambda_{\xi,i}$ and $\xi_{\xi,i}$ are respectively the
¹⁴⁸ mean and standard deviation of the $\ln Y_{ij}$ value necessary to cause the ξ^{th} damage state to occur
¹⁴⁹ or be exceeded for the i^{th} component, and the other variables are defined above.

¹⁵⁰ The California Department of Transportation (Caltrans) provided the fragility function values
¹⁵¹ $\lambda_{\xi,i}$ and $\xi_{\xi,i}$ used for road bridges in this study [30]. The $\lambda_{\xi,i}$ values are based on bridge
¹⁵² characteristics including number of spans and age [27], and the $\xi_{\xi,i}$ values are constant for all
¹⁵³ bridges. The BART seismic safety group provided the fragility function values $\lambda_{\xi,i}$ and $\xi_{\xi,i}$ used
¹⁵⁴ in this study for the BART-related components [31]; data is available for the aerial structures,
¹⁵⁵ primarily in the East Bay, but not tunnels. The BART fragility function values correspond to
¹⁵⁶ the safety performance goals under the recent retrofit program, and both the $\lambda_{\xi,i}$ and $\xi_{\xi,i}$ vary
¹⁵⁷ depending upon the structure's characteristics. Both sets of fragility functions are based on the
¹⁵⁸ assumption that damage can be reasonably accurately estimated by the ground motion intensity
¹⁵⁹ at each site independently, and that the damage state can be reasonably estimated by an analytical
¹⁶⁰ model considering a single ground-motion intensity measure. In addition, the fragility curves
¹⁶¹ do not directly consider the effects of degradation. Current work is ongoing to refine these
¹⁶² assumptions [e.g., 28, 32, 33]. Per ground-motion intensity map, we sample one damage map (e.g.,
¹⁶³ Figure 2b), which has a realization of the component damage state at each component location
¹⁶⁴ according to the fragility function (eq. 2).

¹⁶⁵ **Transit network damage** Each of the 43 transit systems we considered will function differently
¹⁶⁶ when damaged. Because the Caltrain rail system consists of a single set of shared tracks, managers
¹⁶⁷ suggested that the system would either be fully operational, or not at all if even one segment
¹⁶⁸ of the system was non-operational. Similarly, managers suggested modeling the VTA system
¹⁶⁹ as either fully or not at all functional. Depending on where the BART train cars are when the
¹⁷⁰ earthquake strikes, the agency could accommodate different emergency plans. However, BART
¹⁷¹ representatives suggested that if any part of a route is damaged, the entire corresponding route
¹⁷² would not be operational (but other routes on different tracks might be still operational). In other
¹⁷³ words, each BART route as well as the Caltrain and VTA routes are weakest-link systems, so the
¹⁷⁴ failure of a single component will cause the route to be non-operational. We modeled the ferry
¹⁷⁵ systems as fully functioning for all earthquake events. For all earthquake events including the
¹⁷⁶ baseline, trans-bay and cross-county bus lines were discontinued, but main lines in urban areas as
¹⁷⁷ well as other local bus networks were maintained per recommendations from the MTC (though
¹⁷⁸ they face the same delays due to post-disaster traffic congestion as car travelers).

¹⁷⁹ **Road network damage** The damage state of each Caltrans bridge maps directly to the traffic
¹⁸⁰ capacity on associated road segments. Based on discussions with Caltrans, we consider travel
¹⁸¹ conditions one week after an earthquake, since it is a critical period for decision making (for exam-
¹⁸² ple, bridges would have been inspected and surface damage repaired, but major reconstruction
¹⁸³ would not have yet begun). At this point in time, the components are assumed to have either zero
¹⁸⁴ or full traffic capacity [29]. We can thus summarize the component damage using two damage
¹⁸⁵ states, $ds_{damaged}$ (corresponding to HAZUS *extensive* or *complete* damage states) and $ds_{functional}$

186 (*none, slight, or moderate* damage states) [29]. Thus, the functional percentage relationship assigns
187 zero traffic capacity on road segments that have at least one component in the $ds_{damaged}$ damage
188 state, and full traffic capacity otherwise.

189 **III. Network performance**

190 **III.1 Theory**

191 The final step for the event-based risk analysis is to evaluate the network performance measure,
192 X. For this application, we consider mode-destination accessibility change [e.g., 15, 34, 35] (e.g.,
193 Figure 2d). Mode-destination accessibility, hereafter referred to as accessibility, measures the
194 distribution of travel destination opportunities weighted by the composite utility of all modes of
195 travel to those destinations (i.e., the ease of someone getting to different destinations weighted by
196 how desirable those destinations are) [16, 14]. The utility function for the mode-destination choice
197 may be estimated using a multinomial random utility model where the logsum represents the
198 accessibility value [36, 16, 14]. Namely, accessibility for a particular agent a is

$$Acc_a = \ln \left[\sum_{\forall c \in C_a} \exp(V_{a(c)}) \right] \quad (3)$$

199 where $V_{a(c)}$ is the utility of the c^{th} choice for the a^{th} person, and C_a is the choice set for the a^{th}
200 person [16]. Choices refer to travel destinations and the mode of travel (driving, walking, bus, etc.).
201 The units are a dimensionless quantity, *utils*, but can be converted into equivalent time and dollar
202 amounts using *compensating variation* for cost-benefit studies. For the case study, 1 *util* equals
203 the value of 75 minutes or \$20 per person per day [14, 37, 38, 39]. With nearly 7 million people
204 in the study region, even small changes in average *utils* lead to large economic impacts. Since
205 accessibility measures how easily people can get to the destinations they desire, it is a measure a
206 of human welfare [e.g., 14].

207 Once the accessibility network performance measure is computed for each damage map, we
208 aim to estimate the exceedance rate of different levels of performance. The annual rate, λ , of
209 exceeding some threshold of network performance is estimated by summing the occurrence rates
210 of all damage maps in which the performance measure exceeds the threshold:

$$\lambda_{X \geq x} = \sum_{j'=1}^J w_{j'} \mathbb{I}(X_{j'} \geq x) \quad (4)$$

211 where x is an accessibility value threshold of interest and $X_{j'}$ is the accessibility value realization
212 for the j'^{th} damage map. The variable $w_{j'}$ is the occurrence rate of the j'^{th} damage map. The
213 indicator function \mathbb{I} evaluates to 1 if the argument, $X_{j'} \geq x$, is true, and 0 otherwise. By evaluating
214 λ at different threshold values, we derive an exceedance curve.

215 **III.2 Implementation**

216 We compute accessibility using *Travel Model One* (version 0.3), an activity-based model used by the
217 Metropolitan Transportation Commission (MTC), the local metropolitan planning organization
218 (MPO) [40]. It represents the full road network as well as the public transit networks, biking,
219 and walking. Travel demand data consists of the locations of different households in the case
220 study area, their destination preferences and utilities, their number of vehicles, and their income
221 and other demographic data [40, 38, 41]. This data was collected by the MTC from surveys

and census information. We assume that the distributions of travel preferences do not change after an earthquake, although the actual destinations and trips will vary as people choose to forgo trips due to network disruption. The result is a variable-travel-demand model. This model uses a combination of Java code called CT-RAMP [42], and the CitiLabs Cube Voyager and Cube Cluster transportation planning software [40]. The software takes 6+ hours on a high-performance computing platform to analyze a given network state, including reaching equilibrium on users trip choices and preferred travel modes and routes.

Given the computational cost of analyzing the network, analyzing thousands of scenarios with a crude Monte Carlo approach is not feasible. This analysis uses an improved sampling strategy to select damaged networks for analysis, and considers 40 sets of ground-motion intensity maps, damage maps, accessibility performance measure realizations, and corresponding annual rates of occurrence. The 40 realizations were selected (and their occurrence rates adjusted appropriately) using an optimization procedure to ensure that the selected scenarios were consistent with the larger original set of simulations, in terms of the probability distributions of ground motion intensity at individual sites, and other parameters that ensured reasonableness of the distributions of network damage. In this sense, the selected simulations are a “hazard consistent” representation of the distribution of future earthquake impacts that could be experienced in the region. Readers are referred to [17] for more details about this set of events and computing mode-destination accessibility using this model.

241 III. RESULTS AND DISCUSSION

242 I. Region-wide results

243 In this section, we analyze region-wide trends in accessibility losses for the case study area. We
244 first analyze each of the 12 socio-economic groups used in practice for the case study region [38].
245 These socio-economic groups correspond to all combinations of four income classes (Table 1), and
246 three classes of automobile availability in the household (zero automobiles, fewer automobiles
247 than household members that work, as many or more automobiles than household members that
248 work). Each data point for analysis represents a trip by a person of a household from one of these
249 segments, who is modeled as an agent in the transportation model. Expected losses are computed
250 by taking an average of the accessibility losses for people within a given group and region for
251 each earthquake event, weighted by the events’ corresponding occurrence rates. Expected losses
252 for people from each of the 12 groups and 1454 TAZs are shown in Figure 3.

253 In addition to looking at average accessibility loss, we can compute an accessibility exceedance
254 curve for a given group or region. By using equation 4 to compute exceedance rates for multiple
255 accessibility loss thresholds, we can produce results like those in Figure 4. These curves show, for
256 a given group, the annual rate with which a given accessibility decrease will be observed (when
257 considering random future occurrences of earthquakes and damage). Several observations can be
258 made from these results.

259 First, a higher ratio of cars to the number of people who work in a household corresponds
260 to a higher expected decreases in accessibility (as seen by looking across a column in Figure 3).
261 Households with more cars tend to take longer trips, and there is a relationship between needing
262 to travel longer distances and needing an extra car in a household. But there is only a weak
263 trend between average trip length for a TAZ and the predicted impact on accessibility (Figure 5).
264 Instead, we hypothesize that there are other latent variables correlated with both car ownership
265 and accessibility risk (such as geographic location). In Section V, we will further explore the
266 relationship between the percentage of car-based trips and accessibility risk.

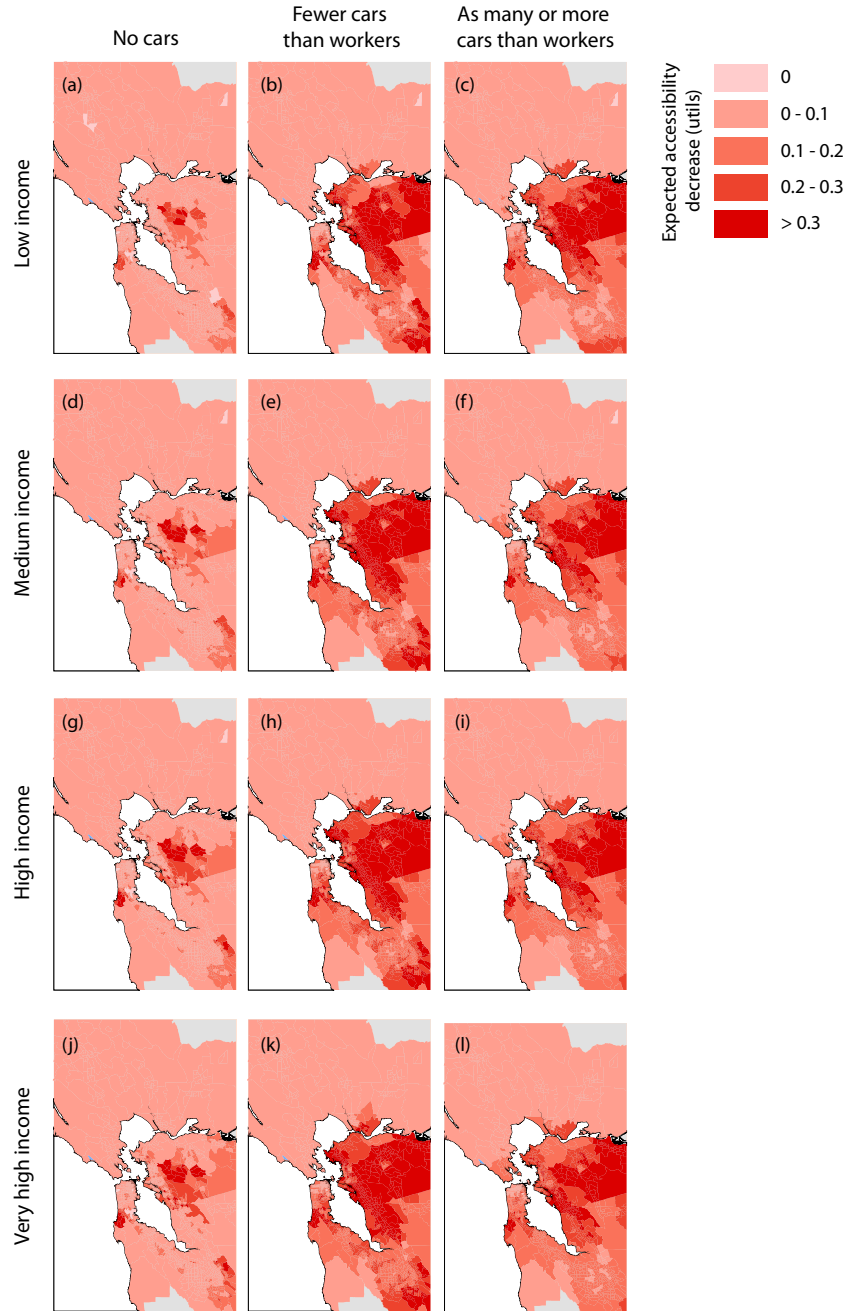


Figure 3: Expected changes in accessibility per person per day for each combination of income class and car ownership group. The darker the color, the greater the losses in accessibility. Each row of figures corresponds to an income class and each column corresponds to a class of car ownership.

267 Second, controlling for car ownership, we see a fairly consistent distribution of risk across
 268 income classes. For example, looking at households with fewer workers than cars (the middle
 269 column of Figure 3), the variation from TAZ to TAZ is much greater than the difference across

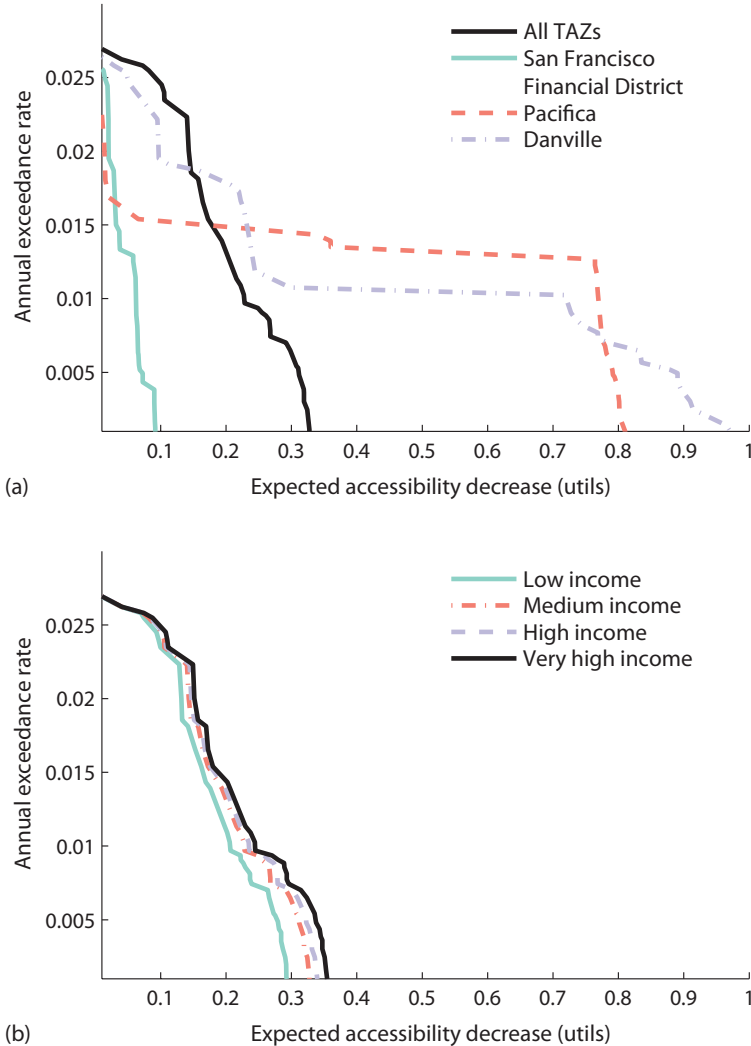


Figure 4: Accessibility annual loss exceedance curve with a comparison by (a) case study TAZs and average over all TAZs and (b) income class; all curves are for medium income households with fewer cars than workers.

income segments. Similarly, while trip lengths are slightly longer for higher income households, the differences are subtle. Thus, for a given TAZ, the differences in impacts across incomes are not that great. There is, however, an unequal geographic distribution of wealth in the study region. Because of this, when we aggregate accessibility risk across TAZs, we see that accessibility risk rises slightly with increasing household income (Figure 4b).

Next, we consider TAZs indicated to have elevated risk. The San Francisco Peninsula is at risk of disruption from large magnitude San Andreas earthquakes, while the East Bay is at risk from slightly smaller but more frequent events on the Hayward Fault. Network simulations indicate that both Hayward and San Andreas earthquakes can cause accessibility problems for the East Bay. Figure 6 shows realizations of a magnitude 6.85 Hayward event and a magnitude 7.45 San

Table 1: Income class definitions for the case study region, as defined by the local planning organization, the MTC [38] and also translated to current 2014 USD using the consumer price index.

Income class	Income range, 1989 USD	Income range, 2014 USD
Low	< \$25,000	< \$47,334
Medium	\$25,000 - \$45,000	\$47,334 - \$85,202
High	\$45,000 - \$75,000	\$85,202 - \$142,004
Very high	> \$75,000	> \$142,004

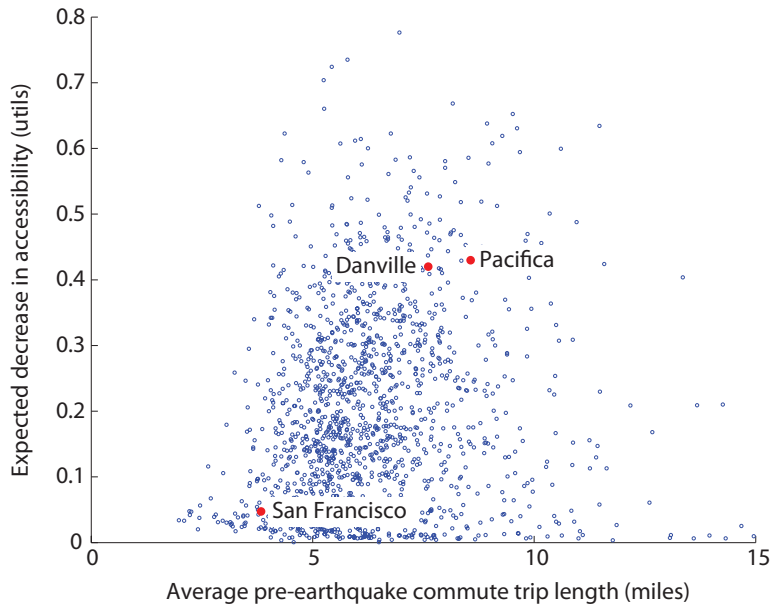


Figure 5: Average pre-earthquake trip length versus change in expected accessibility for all TAZs in the study region. Each dot represents data from one TAZ, and red dots highlight the data points for the three case study communities.

280 Andreas event—both show high accessibility losses in the East Bay. In contrast, the main predicted
 281 accessibility losses in San Francisco correspond primarily to San Andreas events. Figures 6c and 6d
 282 provide one such example. Figures 6e and 6f show a lower magnitude event farther away from
 283 the main population centers: a magnitude 6.35 event in the Great Valley Pittsburg-Kirby Hills
 284 Fault. This shows how the more minor faults in the East Bay can contribute to that area’s risk. The
 285 Figure 6 results are for one specific socio-economic group, but comparable results for the other
 286 groups show the same patterns.

287 Finally, we can examine the rates of loss exceedance (eq. 4), as shown in Figure 4. Recognizing
 288 that the impact varies significantly by TAZ, as indicated by Figure 3, we also examine the
 289 accessibility loss exceedance curve for three communities: part of the San Francisco Financial
 290 District, Danville, and Pacifica. This part of the San Francisco Financial District represents an
 291 area with relatively low expected changes in accessibility, whereas Danville and Pacifica are at an
 292 elevated risk in almost all socio-economic groups (Figure 3). The general trends are corroborated
 293 by the loss exceedance curves for these three communities (Figure 4a shows results for medium
 294 income households with fewer cars than workers). The average middle-class person from Danville
 295 in a household with fewer cars than workers is expected to experience travel-related losses up to 1

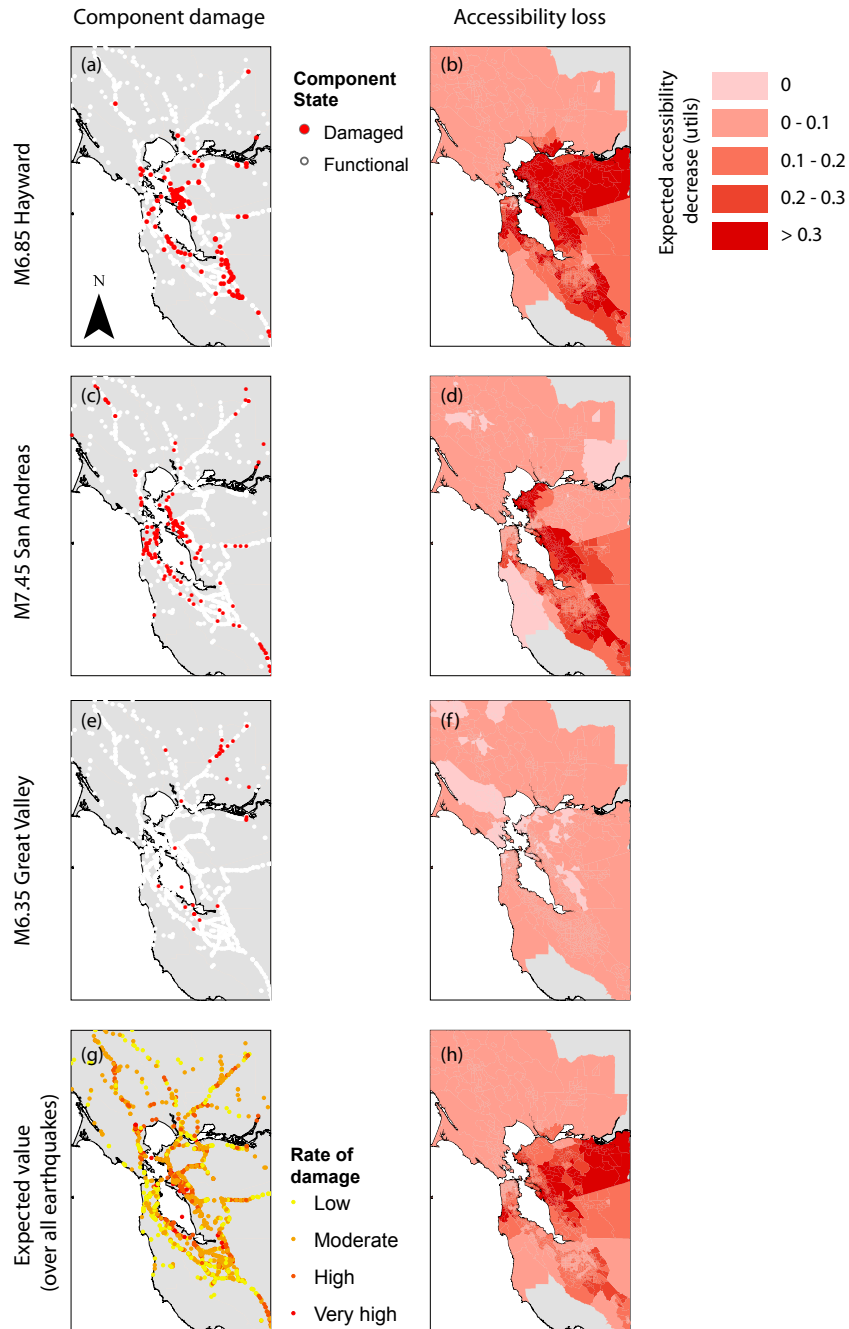


Figure 6: Bridge damage and corresponding accessibility losses by TAZ for medium income households with fewer cars than workers. The top three rows show results from specific events, while the bottom row has expected values calculated as a weighted average over all events.

util (or 75 minutes of extra travel time per day) after a rare earthquake. In contrast, a resident of San Francisco's Financial District has expected losses of only a tenth as much when considering the same exceedance rate. At annual rates of less than 0.01 (i.e., return periods greater than 100

299 years), Danville and Pacifica follow a similar general pattern that differs dramatically from that of
300 San Francisco.

301 **II. Analysis for San Francisco Financial District**

302 Two factors may explain this San Francisco TAZ's lower accessibility losses relative to most other
303 communities. First, it differs dramatically from many other TAZs in having a small percentage of
304 trips made by car (38% versus an average of 85% across all TAZs). Households traveling by foot
305 or bike are less influenced by network damage, because foot travel routes and travel times are
306 assumed to not be affected by bridge damage and road congestion. Additionally, trips by foot and
307 bike tend to be to destinations that are shorter distances away than trips made via other modes.
308 Second, the times for trips to and from work are similar to that of other TAZs, and the average trip
309 distance is only 7% lower than the average for all trips region-wide. So the trip times and lengths
310 do not explain the differences in accessibility losses in this TAZ. The data thus suggests that a
311 major cause for the low accessibility risk of this TAZ is the low dependence on cars for mobility.

312 **III. Analysis for Pacifica**

313 Pacifica is wedged between the Pacific Ocean to the west and the coastal mountains to the east. The
314 main access road is historic California Highway 1, which has a number of older and seismically
315 vulnerable bridges. There are no viable alternative routes to population centers via local roads.
316 Most trips from Pacifica are taken by car (88%), and the average trip length is 108% longer than
317 the region-wide average, so the Highway 1 vulnerability is particularly serious.

318 As a comparison, consider Half Moon Bay, a community about 13 miles to the South (Figure 7).
319 Half Moon Bay has significantly lower expected accessibility losses compared to Pacifica (0.11 *utils*
320 for a middle income household with fewer cars than workers, versus 0.43 *utils* in Pacifica). While
321 the seismic hazard for the two towns is similar, Half Moon Bay's population is about one third of
322 Pacifica's, so there is less local demand for Highway 1's limited road capacity [43]. Perhaps more
323 importantly, Half Moon Bay has a key alternative to California Highway 1: California Highway 92,
324 which links to the main highways of the peninsula. Since Pacifica is unusually reliant on one road
325 with key vulnerabilities, it has an elevated risk for losses in accessibility.

326 **IV. Analysis for Danville**

327 Danville is a suburban community with many residents commuting large distances by car. The
328 average length of a trip from Danville is 85% longer than the average over all trips in the study
329 region, with a relatively high proportion of trips taking more than 60 minutes and traveling over
330 40 miles. These longer trips have more opportunities to be impacted by road closures, because
331 more roads and bridges will be used to complete the trip. Moreover, many Danville trips are via
332 highways, which increases the likelihood of crossing (damage prone) highway bridges.

333 Bridge damage is important for many regions, including Danville, because the percentage
334 of car-based trips is high (85% of all trips from Danville, which is approximately average for
335 all TAZs). For all three simulations shown in Figure 6, some bridges in the Oakland area are
336 damaged and thus closed. In addition, in the first two simulations, there are closures to the north
337 of Danville, which represents one of the two main travel routes from Danville. There are also
338 scattered closed bridges to the west of Danville, a top travel corridor for people of Danville because
339 of the workplace centers in San Francisco, Oakland, and San Jose (all to the west). As for transit, in
340 the first two events, all BART lines are closed, so there are limited alternatives to the popular road
341 routes. The result is that the residents of Danville have reduced access to their normal destinations

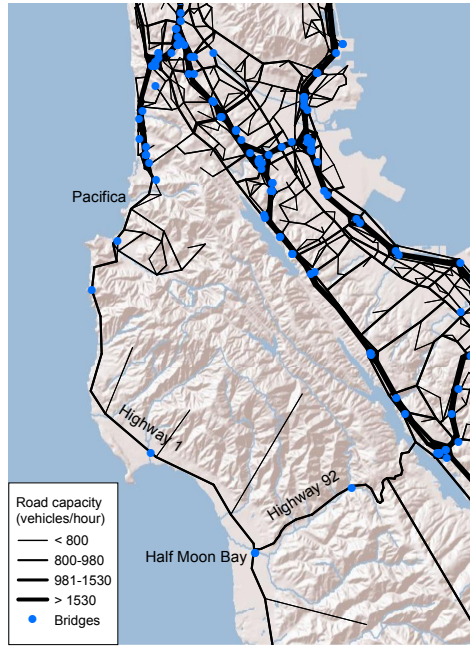


Figure 7: Roads providing access from Pacifica and Half Moon Bay.

after these events. Looking at the rate of bridge damage across all of the earthquake simulations in Figure 6g, we see that bridges in the Oakland area and to the north of Danville are particularly likely to be damaged. This suggests that Danville's proximity to vulnerable bridges contributes to its accessibility risk.

346 V. Impact of travel mode shifts and regional variations in travel mode patterns

347 Over all the simulated events, taking a weighted average by the annual occurrence rate of each
 348 event, we see a 25% reduction in transit ridership after an earthquake. The heavy rail systems
 349 (BART and Caltrain) are not fully operational in most of the forty simulated events (Table 2),
 350 and these have heavy ridership. The light rail systems (VTA and Muni) also suffer losses in
 351 many events (Table 2). Some of the pre-earthquake transit trips do not take place at all in the
 352 post-earthquake simulations, and some switch to other modes (car, foot and bike), causing small
 353 average increases in the number of trips taken by other modes. One exception to this trend is the
 354 M6.35 Great Valley earthquake illustrated in Figure 6e and 6f. In this event, there were no line
 355 closures on the four major transit systems listed in Table 2. There were, however, some bridge
 356 closures on the highways, resulting in a slight increase in transit ridership and in trips by foot.

357 In general, accessibility impact grows with increasing number of damaged transit lines,
 358 particularly in combination with high numbers of damaged bridges (Figure 8). Individual network
 359 simulations also suggest that transit is a key contributor to accessibility risk. For example, the
 360 M6.85 Hayward and the M7.45 Northern San Andreas Fault events from Figure 6 both have around
 361 11% of bridges damaged. These events are labeled in Figure 8, which indicates that the Hayward

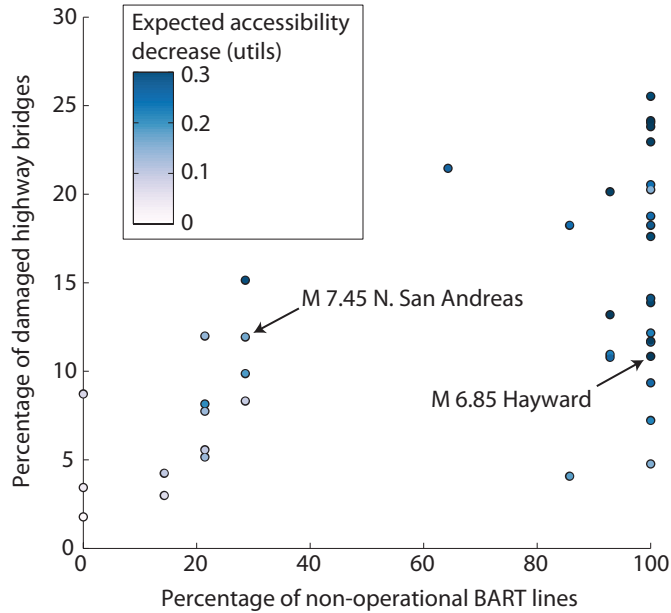


Figure 8: Percentage of BART lines not operational versus percentage of highway bridges damaged, where each data point corresponds to one earthquake simulation. The points are color-coded by the average loss in accessibility per day per person over all TAZs for households with the fewer cars than workers.

Table 2: Number of the 40 earthquake realizations in which for major transit networks have a specified level of functionality. Functionality is measured by the percentage of lines that are operational in a given realization.

Functionality	BART	Caltrain	Muni Light Rail	VTA Light Rail
Full	3	13	25	9
50-99%	10	0	15	0
1-49%	8	0	0	0
None	19	27	0	31

362 event has significantly higher transit network damage and accessibility loss. The Northern San
 363 Andreas event had 10 of the 14 BART lines and all Muni lines operational, whereas the Hayward
 364 event had no BART lines and 5 of the 8 Muni lines operational (Caltrain and VTA were not
 365 operational in either simulation). Moreover, the differences in accessibility results could not have
 366 been predicted from simpler models focusing on bridge portfolio losses, because the percent of
 367 damaged bridges was about the same, and the San Andreas event actually corresponded to a
 368 greater increase in fixed-demand travel time when modeled using a much simpler traffic model.

369 Next, we examine the correlation between a community's walkability, as measured by the
 370 percentage of total trips made by that travel mode, and its expected decrease in accessibility.
 371 Figure 9 shows that communities with a high percentage of pre-earthquake trips on foot have
 372 a lower average decrease in accessibility. This result corroborates the specific example of the
 373 San Francisco Financial District discussed in Section II. Furthermore, on average, the number
 374 of by-foot trips increases after the earthquake events where road congestion worsens. This
 375 model result is consistent with the observations after the 1995 Kobe earthquake [7]. This suggests
 376 that communities with greater walkability are also more resilient to earthquake-related accessibility
 377

378 risk.

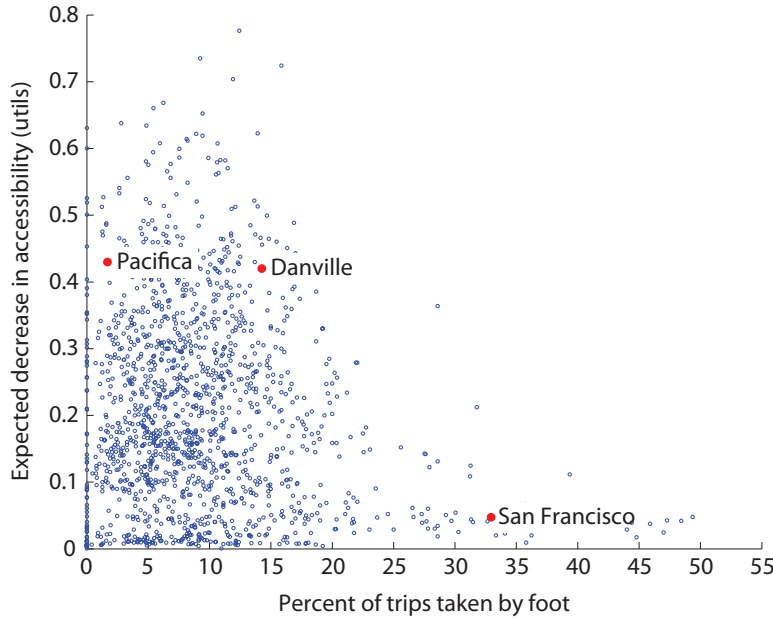


Figure 9: Percentage of pre-earthquake trips taken by foot versus expected decrease in accessibility among households with fewer cars than workers, for all TAZs in the study area. Each dot represents data from one TAZ, and red dots highlight the data points for the three case study communities.

379

IV. CONCLUSIONS

380 We have shown how mode-destination accessibility can be used to link post-earthquake infras-
 381 tructure damage to the impact on human welfare and enables identifying at-risk geographic and
 382 demographic groups in a region. Adopting this performance metric from the urban planning
 383 community, we have illustrated its use for seismic risk assessment and mitigation through a case
 384 study of the San Francisco Bay Area. For the case study, we considered a set of 40 hazard-consistent
 385 earthquake scenarios, ground-motion intensity maps, damage maps, and corresponding annual
 386 rates of occurrence. For each damage map, we performed a detailed activity-based travel model
 387 calculation that includes the road network, transit networks, walking and biking options, variable
 388 travel demand, and mode choice. We used this data and model to compute the mode-destination
 389 accessibility, a performance measure for each community and each socio-economic group (defined
 390 by income class and car ownership).

391 We saw stark differences in accessibility from location to location. We found that these
 392 geographic trends persisted across income classes and car ownership groups. Nonetheless, higher
 393 income households with more cars than workers had higher average accessibility losses than other
 394 socio-economic groups. One reason for this is the geographic clustering of these households in
 395 higher-risk areas. Another factor is that these households tend to take longer daily trips, thus
 396 crossing more roads and bridges and possibly increasing the likelihood of disruption. We also
 397 considered three specific communities that were predicted to have greatly differing experiences
 398 after a future earthquake, in order to understand the geographic and demographic reasons
 399 underlying these differences in risk.

400 This study considered the possibility that travel modes will shift after an earthquake, and
401 communities that can more easily adjust are predicted to experience lower post-earthquake losses
402 in accessibility. The results suggest that the walkability of a community, as measured by the
403 percentage of pre-earthquake trips by foot, is closely linked to reduced accessibility risk. We also
404 found that in almost all of the simulated earthquake events, the transit system is predicted by
405 this model to be severely impacted. The result is a reduced mode share for transit and increased
406 trips by other modes (car, walking, and bike). Thus, this study suggests that neglecting to
407 consider transit disruption can lead to a nonconservative estimate of seismic risk of transportation
408 systems. The model shows, however, that when transit is not damaged—which is rare for this
409 case study—ridership increases.

410 In conclusion, mode-destination accessibility offers important insights into the relationship
411 between damage to physical infrastructure and impacts on human welfare. Using a detailed
412 transportation network model, computationally efficient analysis strategies, and this refined
413 measure of impact, we obtain new insights about users' risk, and obtain metrics that are usable by
414 urban planners responsible for long-term management of transportation systems. This approach
415 provides a foundation for future work in risk mitigation and policy to reduce the vulnerability of
416 at-risk communities. It suggests that initiatives making communities more conducive for cycling
417 and walking to work can increase resiliency to disasters. It also provides a method to quantify
418 economic and societal benefits of upgrading various aspects of a region's transportation systems.

419 **V. ACKNOWLEDGEMENTS**

420 We thank Dave Ory at the Metropolitan Transportation Commission (MTC) and Tom Shantz and
421 Loren Turner at Caltrans for motivating discussions and providing the case study data. The first
422 author thanks the support of the NSF and Stanford Graduate Research Fellowships. This work was
423 supported in part by the National Science Foundation under NSF grant number CMMI 0952402.
424 Any opinions, findings and conclusions or recommendations expressed in this material are those
425 of the authors and do not necessarily reflect the views of the National Science Foundation.

426 **REFERENCES**

- 427 [1] L. Dueñas-Osorio, J. I. Craig, B. J. Goodno, Seismic response of critical interdependent
428 networks, *Earthquake Engineering & Structural Dynamics* 36 (2) (2007) 285–306. doi:10.
429 1002/eqe.626.
- 430 [2] S. E. Chang, M. Shinozuka, J. E. Moore, Probabilistic earthquake scenarios: Extending risk
431 analysis methodologies to spatially distributed systems, *Earthquake Spectra* 16 (3) (2000)
432 557–572. doi:10.1193/1.1586127.
- 433 [3] R. C. Bolin, L. Stanford, *The Northridge earthquake: vulnerability and disaster*, Routledge,
434 London; New York, 1998.
- 435 [4] The World Bank and the United Nations, *Natural hazards, unnatural disasters: the economics*
436 *of effective prevention*, Tech. rep., The World Bank, Washington D.C. (2010).
- 437 [5] California. Dept. of Transportation. Post Earthquake Investigation Team, *Northridge earth-*
438 *quake, 17 January 1994: PEQIT report*, California Department of Transportation, Division of
439 Structures, Sacramento, 1994.

- 440 [6] K. J. Tierney, Business Impacts of the Northridge Earthquake, *Journal of Contingencies and*
441 *Crisis Management* 5 (2) (1997) 87–97. doi:10.1111/1468-5973.00040.
- 442 [7] P. Gordon, H. W. Richardson, B. Davis, Transport-related impacts of the Northridge earth-
443 *quake*, National Emergency Training Center, 1998.
- 444 [8] A. Kiremidjian, J. Moore, Y. Y. Fan, O. Yazlali, N. Basöz, M. Williams, Seismic risk assessment
445 of transportation network systems, *Journal of Earthquake Engineering* 11 (3) (2007) 371–382.
446 doi:10.1080/13632460701285277.
- 447 [9] N. Jayaram, J. W. Baker, Efficient sampling and data reduction techniques for probabilistic
448 seismic lifeline risk assessment, *Earthquake Engineering & Structural Dynamics* 39 (10) (2010)
449 1109–1131. doi:10.1002/eqe.988.
- 450 [10] C. S. Oliveira, M. A. Ferreira, F. M. d. Sá, The concept of a disruption index: application to the
451 overall impact of the July 9, 1998 Faial earthquake (Azores islands), *Bulletin of Earthquake
452 Engineering* 10 (1) (2012) 7–25. doi:10.1007/s10518-011-9333-8.
- 453 [11] P. Bocchini, D. M. Frangopol, Restoration of bridge networks after an earthquake: Multicri-
454 teria intervention optimization, *Earthquake Spectra* 28 (2) (2012) 426–455. doi:10.1193/1.
455 4000019.
- 456 [12] F. Cavalieri, P. Franchin, P. Gehl, B. Khazai, Quantitative assessment of social losses based
457 on physical damage and interaction with infrastructural systems, *Earthquake Engineering &
458 Structural Dynamics* 41 (11) (2012) 1569–1589. doi:10.1002/eqe.2220.
- 459 [13] F. S. Chapin, *Urban land use planning*, University of Illinois Press, 1970.
- 460 [14] D. A. Niemeier, Accessibility: an evaluation using consumer welfare, *Transportation* 24 (4)
461 (1997) 377–396.
- 462 [15] K. T. Geurs, B. van Wee, Accessibility evaluation of land-use and transport strategies: review
463 and research directions, *Journal of Transport Geography* 12 (2) (2004) 127–140. doi:10.1016/
464 j.jtrangeo.2003.10.005.
- 465 [16] S. L. Handy, D. A. Niemeier, Measuring accessibility: an exploration of issues and alternatives,
466 *Environment and Planning A* 29 (7) (1997) 1175–1194.
- 467 [17] M. Miller, Seismic risk assessment of complex transportation networks, PhD thesis, Stanford
468 University (2014).
- 469 [18] M. Miller, J. Baker, Ground-motion intensity and damage map selection for probabilistic infras-
470 tructure network risk assessment using optimization, *Earthquake Engineering & Structural
471 Dynamics* (2014). doi:10.1002/eqe.2506.
- 472 [19] R. Cervero, K.-L. Wu, Polycentrism, commuting, and residential location in the San Francisco
473 Bay area, *Environment and Planning A* 29 (5) (1997) 865–886.
- 474 [20] Y. Han, R. A. Davidson, Probabilistic seismic hazard analysis for spatially distributed
475 infrastructure, *Earthquake Engineering & Structural Dynamics* 41 (15) (2012) 2141–2158.
476 doi:10.1002/eqe.2179.
- 477 [21] E. H. Field, T. H. Jordan, C. A. Cornell, OpenSHA: a developing community-modeling
478 environment for seismic hazard analysis, *Seismological Research Letters* 74 (4) (2003) 406 –
479 419. doi:10.1785/gssrl.74.4.406.

- 480 [22] M. Shinozuka, Y. Murachi, X. Dong, Y. Zhou, M. J. Orlikowski, Effect of seismic retrofit of
481 bridges on transportation networks, *Earthquake Engineering and Engineering Vibration* 2 (2)
482 (2003) 169–179. doi:10.1007/s11803-003-0001-0.
- 483 [23] E. H. Field, T. E. Dawson, K. R. Felzer, A. D. Frankel, V. Gupta, T. H. Jordan, T. Parsons,
484 M. D. Petersen, R. S. Stein, R. J. Weldon, C. J. Wills, Uniform California Earthquake Rupture
485 Forecast, Version 2 (UCERF 2), *Bulletin of the Seismological Society of America* 99 (4) (2009)
486 2053–2107. doi:10.1785/0120080049.
- 487 [24] D. J. Wald, T. I. Allen, Topographic slope as a proxy for seismic site conditions and
488 amplification, *Bulletin of the Seismological Society of America* 97 (5) (2007) 1379–1395.
489 doi:10.1785/0120060267.
- 490 [25] D. M. Boore, G. M. Atkinson, Ground-motion prediction equations for the average horizontal
491 component of PGA, PGV, and 5%-damped PSA at spectral periods between 0.01 s and 10.0 s,
492 *Earthquake Spectra* 24 (1) (2008) 99–138.
- 493 [26] N. Jayaram, J. W. Baker, Correlation model for spatially distributed ground-motion intensities,
494 *Earthquake Engineering & Structural Dynamics* 38 (15) (2009) 1687–1708. doi:10.1002/eqe.
495 922.
- 496 [27] N. Basöz, J. Mander, Enhancement of the highway transportation lifeline module in HAZUS,
497 Tech. rep., Final Pre-Publication Draft (#7) prepared for the National Institute of Building
498 Sciences (NIBS) (1999).
- 499 [28] K. N. Ramanathan, Next generation seismic fragility curves for California bridges incorporating
500 the evolution in seismic design philosophy, PhD thesis, Georgia Institute of Technology
501 (2012).
- 502 [29] S. Werner, C. Taylor, S. Cho, J. Lavoie, REDARS 2 methodology and software for seismic risk
503 analysis of highway systems (technical manual), Tech. rep., Seismic Systems & Engineering
504 Analysis for MCEER, Oakland, CA (2006).
- 505 [30] Caltrans, Caltrans Seismic Design Criteria Version 1.7, Tech. Rep. SDC 1.7, California Depart-
506 ment of Transportation, Sacramento, CA (2013).
- 507 [31] Bechtel/HNTB Team, Design Criteria Volume I, Version 1.2, Tech. rep., San Francisco Bay
508 Area Rapid Transit District, San Francisco Bay Area Rapid Transit District Earthquake Safety
509 Program (2008).
- 510 [32] N. Kurtz, J. Song, P. Gardoni, Time-varying seismic reliability analysis of representative US
511 west coast bridge transportation networks, in: G. Deodatis, B. R. Ellingwood, D. M. Frangopol
512 (Eds.), *Safety, Reliability, Risk and Life-Cycle Performance of Structures and Infrastructures*,
513 CRC Press, 2014, pp. 655–662.
- 514 [33] J. Ghosh, K. Rokneddin, J. E. Padgett, L. Dueñas-Osorio, Seismic reliability assessment of
515 aging highway bridge networks with field instrumentation data and correlated failures. I:
516 Methodology, *Earthquake Spectra* 30 (2) (2013) 795–817. doi:10.1193/040512EQS155M.
- 517 [34] K. Kockelman, Travel Behavior as Function of Accessibility, Land Use Mixing, and Land Use
518 Balance: Evidence from San Francisco Bay Area, *Transportation Research Record: Journal of*
519 *the Transportation Research Board* 1607 (-1) (1997) 116–125. doi:10.3141/1607-16.

- 520 [35] P. Waddell, F. Nourzad, Incorporating nonmotorized mode and neighborhood accessibility in
521 an integrated land use and transportation model system, *Transportation Research Record: Journal of the Transportation Research Board* 1805 (-1) (2002) 119–127. doi:10.3141/1805-14.
- 523 [36] C. F. Manski, Structural analysis of discrete data with econometric applications, MIT Press,
524 1981.
- 525 [37] K. A. Small, H. S. Rosen, Applied welfare economics with discrete choice models, *Econometrica* 49 (1) (1981) 105–130. doi:10.2307/1911129.
- 527 [38] D. Ory, Personal communication (2013).
- 528 [39] United States Department of Transportation, Revised departmental guidance: valuation of
529 travel time in economic analysis, US Department of Transportation, Washington, DC.
- 530 [40] G. Erhardt, P. Brinckerhoff, D. Ory, A. Sarvepalli, J. Freedman, J. Hood, B. Stabler, MTC's
531 Travel Model One: applications of an activity-based model in its first year, in: Innovations in
532 Travel Modeling 2012, Tampa, Florida, 2012, p. 9.
- 533 [41] P. Waddell, UrbanSim: modeling urban development for land use, transportation, and
534 environmental planning, *Journal of the American Planning Association* 68 (3) (2002) 297–314.
535 doi:10.1080/01944360208976274.
- 536 [42] W. Davidson, P. Vovsha, J. Freedman, R. Donnelly, CT-RAMP family of activity-based models,
537 in: Proceedings of the 33rd Australasian Transport Research Forum (ATRF), Canberra,
538 Australia, 2010, p. 15.
- 539 [43] U.S. Bureau of the Census, United States Census 2010, Tech. rep., U.S. Census Bureau,
540 Washington D.C. (2010).